

Effect of counter-rotating terms on the spontaneous emission in an anisotropic photonic crystalShuai Yang,¹ M. Al-Amri,^{1,2,3} Shi-Yao Zhu,³ and M. Suhail Zubairy¹¹*Institute for Quantum Science and Engineering (IQSE) and Department of Physics and Astronomy, Texas A&M University, College Station, Texas 77843, USA*²*The National Center for Mathematics and Physics, KACST, P.O. Box 6086, Riyadh 11442, Saudi Arabia*³*Beijing Computational Science Research Center, Beijing 100084, China*

(Received 20 December 2012; published 15 March 2013)

The spontaneous emission of a two-level atom in an anisotropic photonic crystal is investigated without making use of the rotating wave approximation (RWA). Similar to the RWA case, there exist two characteristic atomic transition frequencies which separate the radiation field from the localized and propagated fields. Unlike the RWA calculation, these two characteristic frequencies are shifted due to a full calculation of the energy shifts.

DOI: [10.1103/PhysRevA.87.033818](https://doi.org/10.1103/PhysRevA.87.033818)

PACS number(s): 42.50.Ct, 32.80.Qk, 42.70.Qs

I. INTRODUCTION

Spontaneous emission is one of the main and fundamental topics in quantum optics. From the fundamental point of view, it is a peculiar phenomenon which shows the quantum nature of the electromagnetic field [1,2]. It leads to many useful applications and still attracts considerable interests. There have been many techniques that can be utilized to modify spontaneous emission. For example, the quantum interference can lead to spontaneous emission suppression, spectral narrowing, population trapping, and the phase control of spontaneous emission [3–7]. The spontaneous emission can also be enhanced and suppressed by tailoring the density of the radiation field modes [8].

Although spontaneous emission depends strongly on the surrounding environment through the density of states and local strength of the electromagnetic modes [9], it is still a bottleneck limiting the performance of devices in various fields. A good way to overcome this problem is to turn to photonic crystal which is a class of materials with composed periodic dielectric structures. They have remarkable capabilities of localizing and guiding electromagnetic radiation that can be used effectively to control spontaneous emission [10–14]. When the atomic transition frequency lies near the photonic band edge, it leads to the appearance of photon-atom bound states [15,16]. It was found out that such a state can be a good means to coherently control spontaneous emission [17] and spectral splitting [18,19].

Various photonic crystal models have been investigated theoretically [13,16,20–24] and experimentally [25–27]. Among these models is the study of the spontaneous emission of a two-level atom within a three-dimensional anisotropic photonic crystal under the rotating-wave approximation (RWA) [13]. The properties of the radiation field, in such a photonic crystal, depend on the relative position of the atomic transition frequency and the band edge of the photonic crystal. It is shown that there exist two characteristic atomic transition frequencies. Here one can see three different and distinct regions: (a) above these two frequencies, the emission is purely a propagating wave, (b) a localized field below them, (c) while it is a purely diffusion field between the two frequencies. Clearly, there is no coexistence of localized and propagating fields. This remark is quite different when it comes to the one-dimensional photonic crystals as they have a

different density of states [15,16]. For an anisotropic band gap structure, the density of state is proportional to $(\omega_k - \omega_c)^{1/2}$. In contrast, it is proportional to $(\omega_k - \omega_c)^{-1/2}$ for an isotropic band gap structure and leads to a singularity at the band edge.

In the present paper, we not only study the usual spontaneous emission of a two level atom that is embedded in a three-dimensional anisotropic photonic crystal but also consider the full counter-rotating terms. The behavior of the emission is similar to the RWA case, i.e., the localized and propagating fields are also separated by two characteristic atomic transition frequencies. However, these two characteristic frequencies are shifted due to the full Lamb shift which is obtained without making use of the RWA. The paper is organized as follows. In Sec. II, we introduce the model and calculate the spontaneous emission of a two level atom in an anisotropic photonic crystal including the counter-rotating terms in the Hamiltonian. In Sec. III, we first discuss the properties of the fields and compare the results with those of just the RWA. Finally we present some concluding remarks in Sec. IV.

II. MODEL AND CALCULATION

We consider a two-level atom coupled to the radiation field in an anisotropic photonic crystal. The excited and ground energy levels of the atom are labeled as $|1\rangle$ and $|0\rangle$, respectively. The band edge frequency ω_c of the photonic crystal is chosen to be near the atomic transition frequency ω_1 . Without making the rotating wave approximation, the full Hamiltonian of the system is

$$\hat{H} = \hbar\omega_1|1\rangle\langle 1| + \sum_k \hbar\omega_k b_k^\dagger b_k + \hbar \sum_k g_k (b_k^\dagger + b_k)(|0\rangle\langle 1| + |1\rangle\langle 0|), \quad (1)$$

where b_k is the annihilation operator of the radiation mode k with frequency ω_k . The atom-field coupling constant $g_k = (\omega_1 d_1 / \hbar) \sqrt{\hbar / 2\epsilon_0 \omega_k} V_0 \mathbf{e}_k \cdot \mathbf{u}_d$. Here d_1 and \mathbf{u}_d are the magnitude and the unit vector of the atomic dipole moment, V_0 is the quantization volume, and \mathbf{e}_k is the polarization unit vector. In order to take into account the counter-rotating terms, we make a unitary transformation $U = e^{iS}$ on the Hamiltonian,

and keep all of the terms to the second order of g_k . Here

$$S = \sum_k \frac{-ig_k}{\omega_k + \omega_1} (b_k^\dagger - b_k)(|0\rangle\langle 1| + |1\rangle\langle 0|). \quad (2)$$

The transformed Hamiltonian takes the form [28,29]

$$\begin{aligned} \hat{H} = & \hbar(\omega_1 + \Delta\omega_{\text{ndy}}^{(1)})|1\rangle\langle 1| + \Delta\omega_{\text{ndy}}^{(0)}|0\rangle\langle 0| + \sum_k \hbar\omega_k b_k^\dagger b_k \\ & + \hbar \sum_k V_k (b_k^\dagger |0\rangle\langle 1| + b_k |1\rangle\langle 0|), \end{aligned} \quad (3)$$

where the nondynamic energy shifts are

$$\Delta\omega_{\text{ndy}}^{(1)} = \sum_k \frac{g_k^2}{\omega_k} \frac{\omega_1(\omega_1 - \omega_k)}{(\omega_k + \omega_1)^2}, \quad (4a)$$

$$\Delta\omega_{\text{ndy}}^{(0)} = \sum_k \frac{g_k^2}{\omega_k} \frac{\omega_1(\omega_1 + \omega_k)}{(\omega_k + \omega_1)^2}, \quad (4b)$$

and

$$V_k = \frac{2\omega_1 g_k}{\omega_k + \omega_1}. \quad (5)$$

Here we have removed the self-energy of the free electron due to the vacuum fluctuations in the nondynamic shifts.

The dispersion relation in an anisotropic photonic crystal is modified by the periodic dielectric structure. An anisotropic band gap structure is formed on the surface of the the first Brillouin zone of the reciprocal lattice space. The band edge is associated with several symmetry-related points \mathbf{k}_0^i . Near each \mathbf{k}_0^i , the dispersion relation can be approximated as

$$\omega_k = \omega_c + A|\mathbf{k} - \mathbf{k}_0^i|^2. \quad (6)$$

The atom is assumed to be initially in the excited state $|1\rangle$ and the radiation field is in the vacuum state. The state vector

of the system at an arbitrary time t is

$$\begin{aligned} |\psi(t)\rangle = & A(t)e^{-i(\omega_1 + \Delta\omega_{\text{ndy}}^{(1)})t} |1, \{0\}\rangle \\ & + \sum_k B_k(t)e^{-i(\omega_k + \Delta\omega_{\text{ndy}}^{(0)})t} |0, \{1_k\}\rangle. \end{aligned} \quad (7)$$

From the Schrödinger equation, we obtain the following differential equations for the amplitudes $A(t)$ and $B_k(t)$:

$$\frac{\partial}{\partial t} A(t) = - \sum_k V_k e^{-i(\omega_k - \omega_1')t} B_k(t), \quad (8a)$$

$$\frac{\partial}{\partial t} B_k(t) = V_k e^{i(\omega_k - \omega_1')t} A(t). \quad (8b)$$

Here $\omega_1' = \omega_1 + \Delta\omega_{\text{ndy}}^{(1)} - \Delta\omega_{\text{ndy}}^{(0)}$ is the shifted atomic transition frequency.

After making the Laplace transform, we obtain the Laplace transform $\tilde{A}(p)$ for the amplitude $A(t)$,

$$\tilde{A}(p) = (p + \Gamma)^{-1}, \quad (9)$$

with

$$\begin{aligned} \Gamma = & \sum_k \frac{V_k^2}{p + i(\omega_k - \omega_1')} \\ = & \frac{(\omega_1 d_1)^2}{16\pi^3 \epsilon_0 \hbar} \int d\mathbf{k} \frac{1}{\omega_k [p + i(\omega_k - \omega_1')]} \left(\frac{2\omega_1}{\omega_1 + \omega_k} \right)^2 \\ & \times \left[1 - \frac{(\mathbf{k} \cdot \mathbf{u}_d)^2}{k^2} \right]. \end{aligned} \quad (10)$$

Here we convert the mode sum over the transverse plane wave into integral, i.e., $\sum_k \rightarrow [V/(2\pi)^3] \int d\mathbf{k}$. Due to the anisotropy, the integration over \mathbf{k} has to be carried out around the direction of each \mathbf{k}_0^j . The angle between the atom dipole vector and the \mathbf{k}_0^j is θ_j . In addition, we can extend the integration over \mathbf{k} to infinity since the frequencies far away from the band edge do not contribute significantly. Detailed calculation is given in Appendix A. We then have

$$\Gamma = \frac{-i\beta^{3/2} 2\omega_1^2 [\sqrt{\omega_c} + 2\sqrt{\omega_1 + \omega_c} + \sqrt{-ip - (\omega_1' - \omega_c)}]}{\sqrt{\omega_1 + \omega_c} (\sqrt{\omega_c} + \sqrt{\omega_1 + \omega_c})^2 [\sqrt{\omega_c} + \sqrt{-ip - (\omega_1' - \omega_c)}] [\sqrt{\omega_1 + \omega_c} + \sqrt{-ip - (\omega_1' - \omega_c)}]^2}, \quad (11)$$

with $\beta^{3/2} = [(\omega_1 d_1)^2 / 8\pi \epsilon_0 \hbar A^{3/2}] \sum_j \sin^2 \theta_j$. Note here that, in order to ensure the integral in the above equation to be meaningful, the phase angle of $\sqrt{-ip - (\omega_1' - \omega_c)}$ has been defined within $(-\pi/2, \pi/2)$.

The amplitude $A(t)$ is given by the inverse Laplace transform,

$$A(t) = \frac{1}{2\pi i} \int_{\sigma-i\infty}^{\sigma+i\infty} A(p) e^{pt} dp = \frac{1}{2\pi i} \int_{\sigma-i\infty}^{\sigma+i\infty} \frac{e^{pt}}{p + \Gamma} dp, \quad (12)$$

where the real number σ is chosen so that all the singularities of the function $A(s)$ lies to the left of the line $s = \sigma$ in the Bromwich integral.

Following the residue theorem, we have

$$\begin{aligned} A(t) = & \sum_j \frac{e^{x_j^{(1)} t}}{F'(x_j^{(1)})} + \sum_j \frac{e^{x_j^{(2)} t}}{G'(x_j^{(2)})} + \frac{1}{2\pi i} \int_{\omega_{1c}^{i-\infty}}^{\omega_{1c}^{i+0}} \frac{e^{xt}}{x - \frac{i\beta^{3/2} 2\omega_1^2 [\sqrt{\omega_c} + 2\sqrt{\omega_1 + \omega_c} - i\sqrt{x + (\omega_1' - \omega_c)}]}{\sqrt{\omega_1 + \omega_c} (\sqrt{\omega_c} + \sqrt{\omega_1 + \omega_c})^2 [\sqrt{\omega_c} - i\sqrt{x + (\omega_1' - \omega_c)}] [\sqrt{\omega_1 + \omega_c} - i\sqrt{x + (\omega_1' - \omega_c)}]^2}} dx \\ & - \frac{1}{2\pi i} \int_{\omega_{1c}^{i-\infty}}^{\omega_{1c}^{i+0}} \frac{e^{xt}}{x - \frac{i\beta^{3/2} 2\omega_1^2 [\sqrt{\omega_c} + 2\sqrt{\omega_1 + \omega_c} + \sqrt{-ix - (\omega_1' - \omega_c)}]}{\sqrt{\omega_1 + \omega_c} (\sqrt{\omega_c} + \sqrt{\omega_1 + \omega_c})^2 [\sqrt{\omega_c} + \sqrt{-ix - (\omega_1' - \omega_c)}] [\sqrt{\omega_1 + \omega_c} + \sqrt{-ix - (\omega_1' - \omega_c)}]^2}} dx. \end{aligned} \quad (13)$$

The details of the calculation are given in Appendix B, where the functions $F(x)$ and $G(x)$ are defined in Eqs. (B2) and (B4), where $x_j^{(1)}$ are the root of the equation $F(x) = 0$ in the region $[\text{Re}(x) > 0$ or $\text{Im}(x) > \omega'_{ic}]$ as shown in Fig. 4(a), and $x_j^{(2)}$ are the root of equation $G(x) = 0$ in the region $[\text{Im}(x) < \omega'_{ic}$ and $\text{Re}(x) < 0]$ as shown in Fig. 4(b).

With the solved atomic amplitudes, the emitted field $\mathbf{E}(\mathbf{r}, t)$ can be calculated as

$$\mathbf{E}(\mathbf{r}, t) = \frac{\omega_1 d_1}{16\pi^3 \epsilon_0} \mathbf{E}_0(\mathbf{r}, t) \iiint e^{-i(\omega_q t - \mathbf{q}\mathbf{r})} \times \left[\int_0^t A(t') e^{i(\omega_q - \omega_1)t'} dt' \right] d\mathbf{q}, \quad (14)$$

where $\mathbf{E}_0(\mathbf{r}, t) = \sum_i e^{i\mathbf{k}_0^i t} [\mathbf{u}_i - \mathbf{k}_0^i (\mathbf{k}_0^i \mathbf{u}_i) / (k_0^i)^2]$.

III. RESULTS

A. Emitted field

As expected from Eq. (13), the dynamical properties of the emitted field is strongly related to roots $x_j^{(1)}$ and $x_j^{(2)}$. We can find from Eqs. (B2) and (B4) that the properties of these roots depend on the relative positions of the upper level of the atom and the band edge. Numerical studies reveal that there exists two characteristic frequencies of the relative positions Ω_1 and Ω_2 ($\Omega_1 < \Omega_2$). In region I ($\omega_1 < \Omega_1$), only one purely imaginary root $x^{(1)}$ exists for $F(x) = 0$ in the contoured area as shown in Fig. 4(a), while there is no root $x^{(2)}$ for $G(x) = 0$ in the contoured area as shown in Fig. 4(b). In region II ($\Omega_1 \leq \omega_1 \leq \Omega_2$), there is no root for both $x^{(1)}$ and $x^{(2)}$ in the defined contoured areas. In region III ($\omega_1 > \Omega_2$), there is no root for $x^{(1)}$, while one and only one complex root with a negative real part exists for $x^{(2)}$. The properties of the roots are the same as in the case when RWA is made. Therefore, upon substituting Eq. (13) into Eq. (14) and following the discussion in Ref. [13], we can write the radiation field as the sum of three parts:

$$\mathbf{E}(\mathbf{r}, t) = \mathbf{E}_l(\mathbf{r}, t) + \mathbf{E}_p(\mathbf{r}, t) + \mathbf{E}_d(\mathbf{r}, t). \quad (15)$$

Here $\mathbf{E}_l(\mathbf{r}, t)$ comes from the purely imaginary root for $x^{(1)}$. Thus it is a localized field which exists only when $\omega_1 < \Omega_1$. The complex root with a negative real part for $x^{(2)}$ results in a propagating field as denoted by $\mathbf{E}_p(\mathbf{r}, t)$. It exists only if $\omega_1 > \Omega_2$. Clearly, the localized field and propagating field can not coexist. The diffusion field $\mathbf{E}_d(\mathbf{r}, t)$ comes from the third and fourth terms in Eq. (13). Note that although the behavior of the radiation field is the same as the case when RWA is assumed, the positions of the two characteristic frequencies Ω_1 and Ω_2 are different. Therefore, the regions of the localized, diffusion, and propagating fields are shifted, as shown in Fig. 1, which will be explained later.

B. Population in the upper level

The evolution of the population in the excited state is

$$P(t) = |A(t)|^2. \quad (16)$$

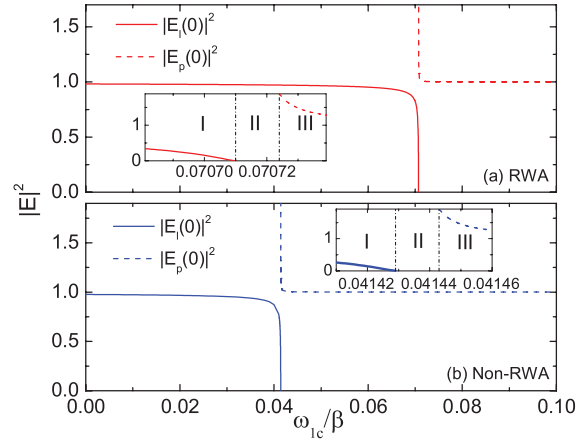


FIG. 1. (Color online) The squared amplitude (in arbitrary units) of the localized mode and the propagating mode as function of detuning of resonant frequency from photonic band edge $\omega_1 c$ with $\omega_c = 200\beta$. The top figure corresponds to the case with RWA. The bottom figure corresponds to the case without making RWA. The three ranges I, II, and III correspond to the localized modes, diffusion modes, and propagating modes, respectively.

As discussed in Ref. [13], the propagating and localized fields cannot coexist in the anisotropic crystal. The diffusion field is negligibly small when propagating or localized field exists. Therefore, there is no interference and the population in the upper level has no quasi-oscillation. If the emission is localized field, it dresses the atoms to form a dressed state and leads to a fractionalized steady-state population in the upper level. If only the diffusion field exists, the upper level decays in the manner of a power law. However, if we have only the propagating field, the upper-level population decays exponentially. If we take into account the effect of the counter-rotating terms, the regions of the localized, diffusion, and propagating fields are shifted with respect to the detuning ω_{1c} , see Fig. 1.

We, therefore, expect a different behavior for the population in the upper level. When $\omega_{1c} = 0.041436\beta$, the detuning lies in region I in Fig. 1(a), while it lies in region II in Fig. 1(b). So if we include the counter-rotating terms in the Hamiltonian, only the diffusion field exists, while RWA predicts a localized field. Consequently, the population in the upper level goes to a constant under RWA, while the non-RWA term leads to a power law decay, see Fig. 2(a). When $\omega_{1c} = 0.055\beta$, the detuning lies in region I in Fig. 1(a), while it lies in region III in Fig. 1(b). Therefore, the emission is localized if we make RWA, while non-RWA terms predict a propagating field. Therefore the population shows different behaviors: nondecaying under RWA and exponentially decaying if RWA is not made, see Fig. 2(b). When $\omega_{1c} = 0.07072\beta$, the detuning lies in region II in Fig. 1(a), while it lies in region III in Fig. 1(b). We expect a diffusion field under RWA and a propagating field without RWA. Correspondingly, the population in the upper level decays polynomially under RWA and exponentially without RWA, see Fig. 2(c).

When time goes to infinity the population in the upper level can survive only if the emission is a localized field. The steady-state atomic population can be obtained

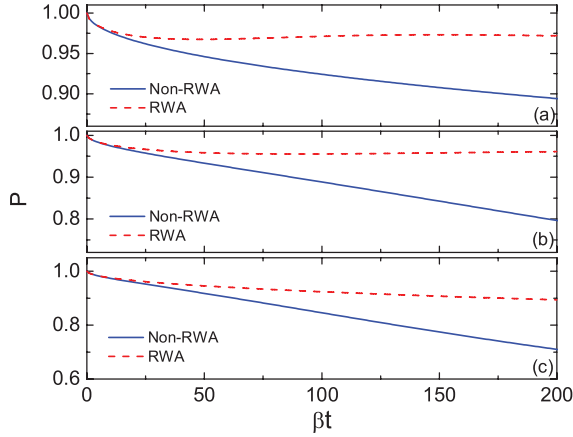


FIG. 2. (Color online) The time evolution of the upper-level population with $\omega_c = 200\beta$. (a) $\omega_{1c} = 0.041436\beta$, (b) $\omega_{1c} = 0.055\beta$, and (c) $\omega_{1c} = 0.07072\beta$, respectively.

as

$$P_{\text{steady}} = \left| \frac{1}{F'(x^{(1)})} \right|^2. \quad (17)$$

We expect, from Fig. 1, that there is a shift of the steady-state population with respect to the detuning ω_{1c} if we consider the effect of the counter-rotating terms, see Fig. 3.

C. Lamb shift

From the dispersion relation Eq. (6), the density of the field modes is 0 for $\omega_k < \omega_c$. So a naive guess could be $\omega_1 = \omega_c$ which is a characteristic point for the behavior of the emission field. If $\omega_1 < \omega_c$, the field should be localized. When $\omega_1 > \omega_c$, the localized field disappears.

However, the strong interaction between the atom and the field shifts the atomic energy levels. When RWA is made, the interaction Hamiltonian is $H_I^{\text{RWA}} = \hbar \sum_k g_k (b_k^\dagger |0\rangle\langle 1| + b_k |1\rangle\langle 0|)$. The second-order perturbation energy shift is

$$\begin{aligned} \Delta E_{\text{RWA}} &= \sum_k \frac{|\langle 0, \{1_k\} | H_I^{\text{RWA}} | 1, \{0\} \rangle|^2}{\hbar(\omega_1 - \omega_k)} \\ &= \sum_k \frac{\hbar g_k^2}{\omega_1 - \omega_k}. \end{aligned} \quad (18)$$

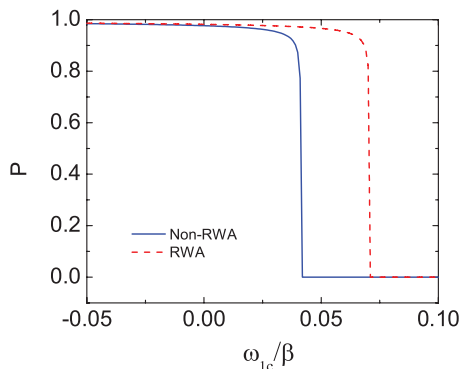


FIG. 3. (Color online) The steady-state atomic population in the upper level with respect to the detuning with $\omega_c = 200\beta$.

When $\omega_1 = \omega_c = 200\beta$, and substitute for ω_k from the dispersion relation in Eq. (6), we obtain this shift $\Delta E_{\text{RWA}} = -0.0707\hbar\beta$. This shift pushes down the actual transition frequency by an amount of 0.0707β (see Appendix C for detailed calculations). Therefore, the field is still localized even if the atomic transition frequency lies above the band edge of the photonic crystal until ω_{1c} exceeds 0.0707β .

However, this energy shift obtained under RWA is not the whole Lamb shift, because it does not include the shift from the counter-rotating terms. When the counter-rotating terms are included in the Hamiltonian, the transformed Hamiltonian contains nondynamic energy shifts. In addition, the interaction constant is rescaled and the interaction Hamiltonian is $H_I = \hbar \sum_k V_k (b_k^\dagger |0\rangle\langle 1| + b_k |1\rangle\langle 0|)$. In this case, the total Lamb shift is given by Refs. [29,31]

$$\begin{aligned} \Delta E_{\text{Lamb}} &= \Delta E_{\text{ndy}} + \Delta E_{\text{dyn}} \\ &= \hbar(\Delta\omega_{\text{ndy}}^{(1)} - \Delta\omega_{\text{ndy}}^{(0)}) + \sum_k \frac{|\langle 0, \{1_k\} | H_I | 1, \{0\} \rangle|^2}{\hbar(\omega_1 - \omega_k)} \\ &= \sum_k \frac{2\hbar g_k^2 \omega_1}{\omega_1^2 - \omega_k^2}. \end{aligned} \quad (19)$$

The shift is $\Delta E_{\text{Lamb}} = -0.0414\hbar\beta$. The frequency difference between the atomic transition and the gap edge $\omega_{1c} \approx 0.0414\beta$, which coincides with Fig. 1(b), is a characteristic frequency for the behavior of the emission field. The Lamb shift due to strong virtual atom-photon interaction results in a peculiar fact that the radiation field is still localized when the atomic frequency is above the band edge of the photonic crystal until the amount of 0.0414β . In the region $0.0414\beta < \omega_{1c} < 0.0707\beta$, the emission is a propagating mode, which would be a localized mode under RWA.

IV. CONCLUSION

In conclusion, we have studied the spontaneous emission of a two-level atom in an anisotropic photonic crystal without making RWA. Similar to the RWA case, there exists two characteristic transition frequencies. Below the two frequencies, the localized field exists while a propagating field shows up above the two frequencies. The localized radiation field exists even if the atomic transition frequency is above the band edge of the photonic crystal. And the localized field cannot coexist with the propagating field. In comparison with the RWA case, the two characteristic frequencies are shifted.

ACKNOWLEDGMENTS

This work is supported by a grant from the King AbdulAziz City for Science and Technology (KACST) and an NPRP grant (4-346-1-061) from Qatar National Research Fund (QNRF). M.A. gratefully acknowledges the hospitality at the Institute for Quantum Science and Engineering (IQSE) and Department of Physics and Astronomy, Texas A&M University.

APPENDIX A: CALCULATION OF Γ

It follows from Eq. (10) that

$$\Gamma = \sum_k \frac{V_k^2}{p + i(\omega_k - \omega'_1)} = \frac{(\omega_1 d_1)^2}{16\pi^3 \epsilon_0 \hbar} \sum_j \int_j d\mathbf{k} \left(\frac{2\omega_1}{\omega_1 + \omega_k} \right)^2 \times \frac{1}{\omega_k} \left[1 - \frac{(\mathbf{k} \cdot \mathbf{u}_d)^2}{k^2} \right] \frac{1}{p - i(\omega'_1 - \omega_k)}. \quad (\text{A1})$$

If the density of a state is broadband, such as in vacuum, the Weisskopf-Wigner approximation is valid and one can use the first-order pole contribution of p to calculate the above integration. However, the density of the electromagnetic modes of the photonic crystal changes rapidly in the vicinity of the band edge, hence, the Weisskopf-Wigner perturbation theory is inadequate. We have to perform an exact integration in

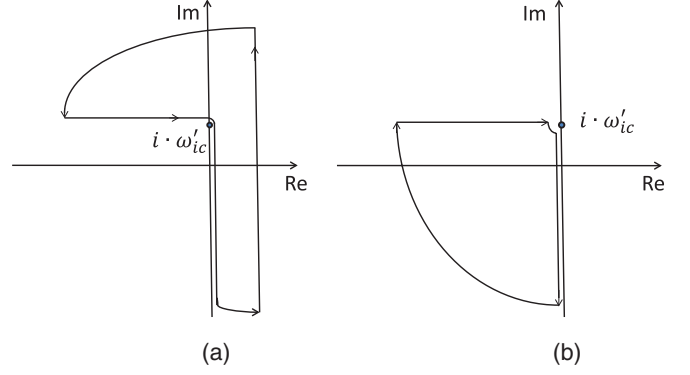


FIG. 4. (Color online) (a) The integration contour of Eq. (B1). (b) The integration contour of Eq. (B3).

Eq. (A1). Therefore we substitute the dispersion relation as described in Eq. (6) in Eq. (A1):

$$\begin{aligned} \Gamma &= \frac{(\omega_1 d_1)^2}{16\pi^3 \epsilon_0 \hbar} \sum_j (\sin \theta_j)^2 \int_j d\mathbf{k} \left(\frac{2\omega_1}{\omega_1 + \omega_c + A|\mathbf{k} - \mathbf{k}_0^i|^2} \right)^2 \frac{1}{\omega_c + A|\mathbf{k} - \mathbf{k}_0^i|^2} \frac{1}{p + iA|\mathbf{k} - \mathbf{k}_0^i|^2 + i(\omega_c - \omega'_1)} \\ &= \frac{(\omega_1 d_1)^2}{16\pi^3 \epsilon_0 \hbar} \sum_j (\sin \theta_j)^2 \int_j d\mathbf{q} \left(\frac{2\omega_1}{\omega_1 + \omega_c + Aq^2} \right)^2 \frac{1}{\omega_c + Aq^2} \frac{1}{p + i(\omega_c - \omega'_1) + iAq^2} \\ &= \frac{(\omega_1 d_1)^2}{4\pi^2 \epsilon_0 \hbar} \sum_j (\sin \theta_j)^2 \int_j dq \left(\frac{2\omega_1}{\omega_1 + \omega_c + Aq^2} \right)^2 \frac{q^2}{\omega_c + Aq^2} \frac{1}{p + i(\omega_c - \omega'_1) + iAq^2} \\ &= -i \frac{(\omega_1 d_1)^2}{4\pi^2 \epsilon_0 \hbar A^{3/2}} \sum_j (\sin \theta_j)^2 \int_j dx \left(\frac{2\omega_1}{\omega_1 + \omega_c + x^2} \right)^2 \frac{x^2}{\omega_c + x^2} \frac{1}{-i(p + i\omega_c - i\omega'_1) + x^2} \\ &= \frac{-i\beta^{3/2} \cdot 2\omega_1^2 [\sqrt{\omega_c} + 2\sqrt{\omega_1 + \omega_c} + \sqrt{-ip - (\omega'_1 - \omega_c)}]}{\sqrt{\omega_1 + \omega_c} (\sqrt{\omega_c} + \sqrt{\omega_1 + \omega_c})^2 [\sqrt{\omega_c} + \sqrt{-ip - (\omega'_1 - \omega_c)}] [\sqrt{\omega_1 + \omega_c} + \sqrt{-ip - (\omega'_1 - \omega_c)}]^2}. \quad (\text{A2}) \end{aligned}$$

APPENDIX B: THE INVERSE LAPLACE TRANSFORM

According to Eq. (12), we proceed the inverse Laplace transform as follows. Since $\sqrt{-ix - (\omega'_1 - \omega_c)}$ is not single valued, we cut the complex plane along $(\omega'_1 i, -\infty i)$. We then choose the integration contour as shown in Fig. 4(a). According to the residue theorem,

$$A(t) = \sum_j \frac{e^{x_j^{(1)} t}}{F'(x_j^{(1)})} - \frac{1}{2\pi i} \left[\int_{\omega'_1 i - \infty}^{\omega'_1 i + 0} + \int_{\omega'_1 i + 0}^{-\infty i + 0} \right] \frac{e^{xt}}{x + \Gamma} dx, \quad (\text{B1})$$

where

$$\begin{aligned} F(x) &\equiv x - \{i\beta^{3/2} 2\omega_1^2 [\sqrt{\omega_c} + 2\sqrt{\omega_1 + \omega_c} + \sqrt{-ix - (\omega'_1 - \omega_c)}]\} \{ \sqrt{\omega_1 + \omega_c} (\sqrt{\omega_c} + \sqrt{\omega_1 + \omega_c})^2 \\ &\quad \times [\sqrt{\omega_c} + \sqrt{-ix - (\omega'_1 - \omega_c)}] [\sqrt{\omega_1 + \omega_c} + \sqrt{-ix - (\omega'_1 - \omega_c)}]^2 \}^{-1}, \quad (\text{B2}) \end{aligned}$$

$$F'(x) = \frac{dF}{dx},$$

and $x_j^{(1)}$ is the root of the equation $F(x) = 0$ in the region as the contour shown in Fig. 4(a). The last term of Eq. (B1) can be calculated as follows:

$$\begin{aligned} \frac{1}{2\pi i} \int_{\omega'_{1c}i+0}^{-\infty i+0} \frac{e^{xt}}{x + \Gamma} dx &= \frac{1}{2\pi i} \int_{\omega'_{1c}i+0}^{-\infty i+0} \frac{e^{xt}}{x - \frac{i\beta^{3/2}2\omega_1^2[\sqrt{\omega_c} + 2\sqrt{\omega_1 + \omega_c} + \sqrt{-ix - (\omega'_1 - \omega_c)}]}{\sqrt{\omega_1 + \omega_c}(\sqrt{\omega_c} + \sqrt{\omega_1 + \omega_c})^2[\sqrt{\omega_c} + \sqrt{-ix - (\omega'_1 - \omega_c)}][\sqrt{\omega_1 + \omega_c} + \sqrt{-ix - (\omega'_1 - \omega_c)}]^2}} dx \\ &= \frac{1}{2\pi i} \int_{\omega'_{1c}i}^{-\infty i} \frac{e^{xt}}{x - \frac{i\beta^{3/2}2\omega_1^2[\sqrt{\omega_c} + 2\sqrt{\omega_1 + \omega_c} - i\sqrt{ix + (\omega'_1 - \omega_c)}]}{\sqrt{\omega_1 + \omega_c}(\sqrt{\omega_c} + \sqrt{\omega_1 + \omega_c})^2[\sqrt{\omega_c} - i\sqrt{ix + (\omega'_1 - \omega_c)}][\sqrt{\omega_1 + \omega_c} - i\sqrt{ix + (\omega'_1 - \omega_c)}]^2}} dx \\ &= -\sum_j \frac{e^{x_j^{(2)}t}}{G'(x_j^{(2)})} - \frac{1}{2\pi i} \int_{\omega'_{1c}i-\infty}^{\omega'_{1c}i+0} \frac{e^{xt}}{x - \frac{i\beta^{3/2}2\omega_1^2[\sqrt{\omega_c} + 2\sqrt{\omega_1 + \omega_c} - i\sqrt{ix + (\omega'_1 - \omega_c)}]}{\sqrt{\omega_1 + \omega_c}(\sqrt{\omega_c} + \sqrt{\omega_1 + \omega_c})^2[\sqrt{\omega_c} - i\sqrt{ix + (\omega'_1 - \omega_c)}][\sqrt{\omega_1 + \omega_c} - i\sqrt{ix + (\omega'_1 - \omega_c)}]^2}} dx, \end{aligned} \quad (\text{B3})$$

where

$$\begin{aligned} G(x) &\equiv x - \{i\beta^{3/2}2\omega_1^2[\sqrt{\omega_c} + 2\sqrt{\omega_1 + \omega_c} - i\sqrt{ix + (\omega'_1 - \omega_c)}]\}\{\sqrt{\omega_1 + \omega_c}(\sqrt{\omega_c} + \sqrt{\omega_1 + \omega_c})^2 \\ &\quad \times [\sqrt{\omega_c} - i\sqrt{ix + (\omega'_1 - \omega_c)}][\sqrt{\omega_1 + \omega_c} - i\sqrt{ix + (\omega'_1 - \omega_c)}]^2\}^{-1}, \\ G'(x) &= \frac{dG}{dx}, \end{aligned} \quad (\text{B4})$$

and $x_j^{(2)}$ is the root of the equation $G(x) = 0$ in the region as the contour shown in Fig. 4(b). Note that in Eq. (B3), we integrate along the left edge of $(\omega'_{1c}i, -\infty i)$ instead of the right edge. Thus, $\sqrt{-ix - (\omega'_1 - \omega_c)}$ turns to $-i\sqrt{ix + (\omega'_1 - \omega_c)}$.

From Eqs. (B1) and (B3), we then have

$$\begin{aligned} A(t) &= \sum_j \frac{e^{x_j^{(1)}t}}{F'(x_j^{(1)})} + \sum_j \frac{e^{x_j^{(2)}t}}{G'(x_j^{(2)})} + \frac{1}{2\pi i} \int_{\omega'_{1c}i-\infty}^{\omega'_{1c}i+0} \frac{e^{xt}}{x - \frac{i\beta^{3/2}2\omega_1^2[\sqrt{\omega_c} + 2\sqrt{\omega_1 + \omega_c} - i\sqrt{ix + (\omega'_1 - \omega_c)}]}{\sqrt{\omega_1 + \omega_c}(\sqrt{\omega_c} + \sqrt{\omega_1 + \omega_c})^2[\sqrt{\omega_c} - i\sqrt{ix + (\omega'_1 - \omega_c)}][\sqrt{\omega_1 + \omega_c} - i\sqrt{ix + (\omega'_1 - \omega_c)}]^2}} dx \\ &\quad - \frac{1}{2\pi i} \int_{\omega'_{1c}i-\infty}^{\omega'_{1c}i+0} \frac{e^{xt}}{x - \frac{i\beta^{3/2}2\omega_1^2[\sqrt{\omega_c} + 2\sqrt{\omega_1 + \omega_c} + \sqrt{-ix - (\omega'_1 - \omega_c)}]}{\sqrt{\omega_1 + \omega_c}(\sqrt{\omega_c} + \sqrt{\omega_1 + \omega_c})^2[\sqrt{\omega_c} + \sqrt{-ix - (\omega'_1 - \omega_c)}][\sqrt{\omega_1 + \omega_c} + \sqrt{-ix - (\omega'_1 - \omega_c)}]^2}} dx. \end{aligned} \quad (\text{B5})$$

APPENDIX C: ENERGY SHIFTS

The total Lamb shift for a level i , composed of the nondynamic energy shift and the dynamic energy shift, is given by Ref. [29]

$$\begin{aligned} \Delta E_{\text{Lamb}}^i &= \Delta E_{\text{ndy}}^i + \Delta E_{\text{dyn}}^i \\ &= \sum_k \sum_{j \neq i} \frac{\hbar g_k^2 \omega_{ji}(\omega_{ji} + \omega_k)}{\omega_k (\omega_k + |\omega_{ji}|)^2} + \sum_k \sum_{j < i} \frac{4\omega_{ij}^2}{(\omega_{ij} + \omega_k)^2} \frac{\hbar g_k^2}{\omega_{ij} - \omega_k} \\ &= \sum_k \sum_{j \neq i} \frac{\hbar g_k^2 \omega_{ij}}{\omega_k \omega_{ij} - \omega_k}. \end{aligned} \quad (\text{C1})$$

As for the two-level atom in the photonic crystal, $\omega_k = \omega_c + A|\mathbf{k} - \mathbf{k}_0|^2$. When $\omega_1 = \omega_c = 200\beta$, the nondynamic energy shift is given by

$$\begin{aligned} \Delta E_{\text{ndy}} &= \hbar(\Delta\omega_{\text{ndy}}^{(1)} - \Delta\omega_{\text{ndy}}^{(0)}) = \sum_k \frac{\hbar g_k^2}{\omega_k} \left[\frac{-\omega_1(-\omega_1 + \omega_k)}{(\omega_k + \omega_1)^2} - \frac{\omega_1(\omega_1 + \omega_k)}{(\omega_k + \omega_1)^2} \right] = -\sum_k \frac{2\hbar g_k^2 \omega_1}{(\omega_k + \omega_1)^2} \\ &= -\frac{\hbar(\omega_1 d_1)^2}{16\pi^3 \epsilon_0 \hbar} \int d\mathbf{k} \left[1 - \frac{(\mathbf{k} \cdot \mathbf{u}_d)^2}{k^2} \right] \frac{2\omega_1}{\omega_k(\omega_1 + \omega_k)^2} \\ &= -\frac{\hbar(\omega_1 d_1)^2}{4\pi^2 \epsilon_0 \hbar} \sum_j \sin^2 \theta_j \int dq \frac{2\omega_1 q^2}{(\omega_c + Aq^2)(\omega_1 + \omega_c + Aq^2)^2} \\ &= -\frac{\hbar\beta^{3/2}}{\pi} \int dx \frac{4\omega_1 x^2}{(\omega_c + x^2)(\omega_1 + \omega_c + x^2)^2} = -0.0085\hbar\beta. \end{aligned} \quad (\text{C2})$$

Here $x = \sqrt{A}q$.

The dynamic shift is given by

$$\Delta E_{\text{dyn}} = \sum_k \frac{4\omega_1^2}{(\omega_1 + \omega_k)^2} \frac{\hbar g_k^2}{\omega_1 - \omega_k} = \frac{\hbar \beta^{3/2}}{\pi} \int dx \frac{8\omega_1^2 x^2}{(\omega_c + x^2)(\omega_1 + \omega_c + x^2)^2(\omega_1 - \omega_c - x^2)} = -0.0328\hbar\beta. \quad (\text{C3})$$

Similarly, the total Lamb shift is

$$\begin{aligned} \Delta E_{\text{Lamb}} &= \sum_k \frac{\hbar g_k^2}{\omega_k} \left(\frac{\omega_1}{\omega_1 - \omega_k} - \frac{-\omega_1}{-\omega_1 - \omega_k} \right) = \sum_k \frac{2g_k^2 \omega_1}{\omega_1^2 - \omega_k^2} \\ &= \frac{\hbar \beta^{3/2}}{\pi} \int dx \frac{4\omega_1 x^2}{(\omega_c + x^2)(\omega_1 + \omega_c + x^2)(\omega_1 - \omega_c - x^2)} = -0.0414\hbar\beta. \end{aligned} \quad (\text{C4})$$

If the RWA is made, one cannot get the full Lamb shift. Specifically, there is no nondynamic shift, and the dynamic shift is

$$\Delta E_{\text{RWA}} = \sum_k \frac{\hbar g_k^2}{\omega_1 - \omega_k} = \frac{\beta^{3/2}}{\pi} \int dx \frac{2x^2}{(\omega_c + x^2)(\omega_1 - \omega_c - x^2)}. \quad (\text{C5})$$

-
- [1] E. M. Purcell, *Phys. Rev.* **69**, 681 (1946).
[2] M. O. Scully and M. S. Zubairy, *Quantum Optics* (Cambridge University Press, Cambridge, 1997).
[3] S.-Y. Zhu and M. O. Scully, *Phys. Rev. Lett.* **76**, 388 (1996).
[4] P. Zhou and S. Swain, *Phys. Rev. Lett.* **77**, 3995 (1996).
[5] C. H. Keitel, *Phys. Rev. Lett.* **83**, 1307 (1999).
[6] G. S. Agarwal, *Phys. Rev. Lett.* **84**, 5500 (2000).
[7] E. Paspalakis and P. L. Knight, *Phys. Rev. Lett.* **81**, 293 (1998).
[8] *Cavity Quantum Electrodynamics*, edited by P. R. Berman, Advances in Atomic, Molecular, and Optical Physics, Supplement (Academic, New York, 1994).
[9] P. Selenyi, *Phys. Rev.* **56**, 477 (1939).
[10] D. C. Allan, J. A. West, J. C. Fajardo, M. T. Gallagher, K. W. Koch, and N. F. Borrelli, in *Photonic Crystal and Light Localization in the 21st Century*, edited by C. M. Soukoulis (Kluwer Academic, Dordrecht, Netherlands, 2001).
[11] P. Russell, *Science* **299**, 358 (2003).
[12] J. D. Joannopoulos, R. D. Meade, and J. N. Winn, *Photonic Crystals* (Princeton, University Press, Princeton, NJ, 1995).
[13] Y. Yang and S.-Y. Zhu, *Phys. Rev. A* **62**, 013805 (2000).
[14] I. Takahashi and K. Ujihara, *Phys. Rev. A* **56**, 2299 (1997).
[15] S. John and J. Wang, *Phys. Rev. Lett.* **64**, 2418 (1990); *Phys. Rev. B* **43**, 12772 (1991).
[16] S. John and T. Quang, *Phys. Rev. Lett.* **74**, 3419 (1995); **76**, 1320 (1996); **78**, 1888 (1997).
[17] T. Quang, M. Woldeyohannes, S. John, and G. S. Agarwal, *Phys. Rev. Lett.* **79**, 5238 (1997).
[18] S. John and T. Quang, *Phys. Rev. A* **50**, 1764 (1994).
[19] Y. P. Yang, S.-Y. Zhu, and M. S. Zubairy, *Opt. Commun.* **166**, 79 (1999).
[20] I. Alvarado-Rodriguez, P. Halevi, and A. S. Sanchez, *Phys. Rev. E* **63**, 056613 (2001).
[21] Y. Yang and S.-Y. Zhu, *Phys. Rev. A* **61**, 043809 (2000).
[22] Y. Yang, M. Fleischhauer, and Shi-Yao Zhu, *Phys. Rev. A* **68**, 043805 (2003).
[23] N. Vats, S. John, and K. Busch, *Phys. Rev. A* **65**, 043808 (2002).
[24] K. Sakoda, *Phys. Rev. B* **55**, 15345 (1997).
[25] S. Noda, K. Tomoda, N. Yamamoto, and A. Chutinan, *Science* **289**, 604 (2000).
[26] S. Noda, M. Fujita, and T. Asano, *Nature Photon.* **1**, 449 (2007).
[27] M. Fujita, S. Takahashi, Y. Tanaka, T. Asano, and S. Noda, *Science* **308**, 1296 (2005).
[28] H. Zheng, S.-Y. Zhu, and M. S. Zubairy, *Phys. Rev. Lett.* **101**, 200404 (2008).
[29] Z.-H. Li, D.-W. Wang, H. Zheng, S.-Y. Zhu, and M. S. Zubairy, *Phys. Rev. A* **80**, 023801 (2009).
[30] Z.-H. Li, D.-W. Wang, H. Zheng, S.-Y. Zhu, and M. S. Zubairy, *Phys. Rev. A* **82**, 050501(R) (2010).
[31] S. Yang, H. Zheng, R. Hong, S.-Y. Zhu, and M. S. Zubairy, *Phys. Rev. A* **81**, 052501 (2010).